

Strain sensitivity control of fiber Bragg grating structures with fused tapers

Orlando Frazão,^{1,2,*} Susana F. O. Silva,^{1,2} Ariel Guerreiro,^{1,2} José L. Santos,^{1,2} Luis A. Ferreira,¹ and Francisco M. Araújo¹

¹Instituto de Engenharia de Sistemas e Computadores do Porto, Rua do Campo Alegre 687, 4169-007 Porto, Portugal

²Departamento de Física, Faculdade de Ciências, Universidade do Porto, Rua do Campo Alegre 687, 4169-007 Porto, Portugal

*Corresponding author: ofraza@inescporto.pt

Received 28 August 2007; revised 4 October 2007; accepted 30 October 2007;
posted 1 November 2007 (Doc. ID 86977); published 13 December 2007

We report on the analysis and experimental validation of the strain sensitivity dependences of a fiber Bragg grating written in standard optical fiber when combined with fused tapers. By controlling the difference between the cross sections of the fused taper and the Bragg grating, the strain sensitivity of the Bragg wavelength can be changed by acting on the gauge length. The strain sensing characteristics of an interferometric structure formed by fabricating a fused taper in the middle of a fiber Bragg grating are also reported. © 2007 Optical Society of America
OCIS codes: 060.0060, 060.2370, 060.3735.

1. Introduction

Over the past decade, fiber Bragg gratings (FBGs) have been used as sensing elements for a large range of measurands (strain, temperature, vibration, pressure, acceleration, etc.) and exploited in specific engineering applications [1]. In particular, FBGs have been widely used in civil engineering and a number of companies have been developing FBG-based sensing systems as alternative solutions to the utilization of electrical sensors [2]. When compared with electric sensors, fiber grating sensors exhibit a number of advantages, such as immunity to electromagnetic interference, a wide temperature operation range, and an inherent wavelength multiplexing capability. A limitation of this type of sensor is the Bragg wavelength cross sensitivity to both strain and temperature, which means it is not always accurate in obtaining independent measurements of these two parameters [3].

Several authors have proposed and demonstrated different sensing head geometries that change the strain sensitivity. James *et al.* [4] proposed a concept

to discriminate strain and temperature through a sensing head configuration based on a splice made between two fibers with different diameters. Other approaches were presented for sensing heads based on twisting a FBG over a second one that remains tensioned [5], or using a chirped Bragg grating fabricated in a fused fiber taper [6]. This one presents some difficulties when dealing with the interrogation of the chirped taper FBG. Due to the taper profile, a complex spectral response is obtained. The bandwidth of the chirped FBG is large and simultaneously triangular, presenting many sidelobes. When strain is applied, the spectral response changes significantly and the wavelength becomes difficult to measure. Conversely, these types of sensing head are interesting when the wavelength is converted into optical intensity. This concept has been studied by Xu *et al.* [7], who presented a temperature-independent strain sensor based on a single FBG written in a taper made by etching. Weichong *et al.* [8] proposed a fiber grating tapered cavity sensor for temperature-independent strain measurement. The taper is located between two gratings, creating two spectral peaks, with their wavelength position changing linearly when strain is applied, but insensitive to temperature variations.

The insertion of a fused taper between two long period gratings (LPGs) was also applied and demonstrated for refractive index measurement. This sensor is efficient in improving and tailoring the sensitivity of the sensing head when it is used for liquid refractive index measurements [9]. This is an example of the possibilities opened for sensing when structures combining fused tapers and fiber gratings (FBGs and LPGs) are explored.

A temperature-independent strain sensor using Bragg gratings embedded in glass tubes was proposed by Song *et al.* [10] and Spirin *et al.* [11]. One of the gratings is placed inside the silica capillary that made it almost strain insensitive. The configuration can be changed using the combination tapers with a capillary tube for measurement of multiparameters.

We propose to use a single FBG in series with a fused taper to make the strain sensitivity of the Bragg grating resonant wavelength dependent on the strain gauge length. We demonstrate that it is feasible to tailor the sensitivity to any value below the standard one associated with a uniform 125 μm diameter silica optical fiber. The strain sensing characteristics of an interferometric structure formed by fabricating a fused taper in the middle of a FBG are also investigated.

2. Principle

Figure 1 shows a schematic of the sensor element. The sensing head is composed of a single FBG sensor in series with a fused taper. The strain gauge of the sensing head has a total length of $L_{\text{total}} = L_{\text{FBG}} + L_{\text{taper}} + L_{\text{fiber}}$. If strain is applied at a constant temperature to the FBG, the central Bragg wavelength (λ_{FBG}) will shift according to

$$\Delta\lambda_{\text{FBG}} = \kappa_{\varepsilon(\text{FBG})} \varepsilon_{\text{FBG}}, \quad (1)$$

where $\kappa_{\varepsilon(\text{FBG})}$ is a constant that depends on the fiber diameter and material, ε_{FBG} is the applied strain, and $\Delta\lambda_{\text{FBG}}$ is the Bragg wavelength shift. If the strain is applied to the entire sensor then an unequal load of stress will appear along each section of the sensor depending on the local mechanical resistance. In particular, the strain loads applied to the FBG and the fused taper are related according to

$$\Delta\varepsilon_{\text{FBG}} EA_{\text{FBG}} = \Delta\varepsilon_{\text{taper}} EA_{\text{taper}}, \quad (2)$$

where E is the Young modulus of the sensor material and A_{FBG} and A_{taper} are the cross-sectional areas in the FBG and in the fused taper regions, respectively. We have assumed that the mechanical properties of the

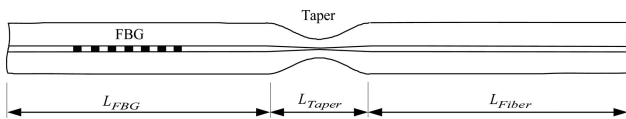


Fig. 1. Schematic of the sensing head based on a single FBG in series with a fused taper.

material in both the FBG and the fused taper regions are the same. Consequently, the strains applied to the two sensor regions depend only on the ratio of the claddings diameters, according to

$$\frac{\varepsilon_{\text{FBG}}}{\varepsilon_{\text{taper}}} = \left(\frac{d_{\text{taper}}}{d_{\text{FBG}}} \right)^2, \quad (3)$$

where d_{FBG} and d_{taper} are the cladding diameters of the FBG and the taper, respectively. The longitudinal strain of the FBG, the fused taper, and piece of fiber are given by

$$\varepsilon_{\text{FBG}} = \frac{\Delta L_{\text{FBG}}}{L_{\text{FBG}}}, \quad \varepsilon_{\text{taper}} = \frac{\Delta L_{\text{taper}}}{L_{\text{taper}}}, \quad \varepsilon_{\text{fiber}} = \frac{\Delta L_{\text{fiber}}}{L_{\text{fiber}}}, \quad (4)$$

where L_{FBG} , L_{taper} , and L_{fiber} , are the lengths of each sensor section and ΔL_{FBG} , ΔL_{taper} , and ΔL_{fiber} , are the corresponding extensions. By definition, the total longitudinal strain of the sensing head, ε , is given by

$$\varepsilon = \frac{\Delta L_{\text{FBG}} + \Delta L_{\text{taper}} + \Delta L_{\text{fiber}}}{L_{\text{FBG}} + L_{\text{taper}} + L_{\text{fiber}}}. \quad (5)$$

Combining Eqs. (3)–(5) and assuming that the diameter of the fiber piece is identical to the one of the FBG (thus having the same local strain), it is possible to derive the relationship between the strain applied to the entire sensor and the strain experienced by the FBG as

$$\varepsilon_{(\text{FBG})} = \frac{L_{\text{FBG}} + L_{\text{taper}} + L_{\text{fiber}}}{L_{\text{FBG}} + L_{\text{taper}} \left(\frac{d_{\text{FBG}}}{d_{\text{taper}}} \right)^2 + L_{\text{fiber}}} \varepsilon. \quad (6)$$

Substituting Eq. (6) into Eq. (1), the Bragg wavelength shift can be rewritten as

$$\Delta\lambda_{\text{FBG}} = \kappa_{\varepsilon(\text{FBG})} \frac{L_{\text{FBG}} + L_{\text{taper}} + L_{\text{fiber}}}{L_{\text{FBG}} + L_{\text{taper}} \left(\frac{d_{\text{FBG}}}{d_{\text{taper}}} \right)^2 + L_{\text{fiber}}} \varepsilon. \quad (7)$$

If the sensing head has N fused tapers along the fiber, Eq. (7) can be generalized, yielding

$$\Delta\lambda_{\text{FBG}} = \kappa_{\varepsilon(\text{FBG})} \frac{L_{\text{FBG}} + \sum_{i=1}^N L_{\text{taper}_i} + L_{\text{fiber}}}{L_{\text{FBG}} + \sum_{i=1}^N L_{\text{taper}_i} \left(\frac{d_{\text{FBG}}}{d_{\text{taper}_i}} \right)^2 + L_{\text{fiber}}} \varepsilon. \quad (8)$$

Equation (7) can also be written as

$$\Delta\lambda_{\text{FBG}} = \kappa_{\varepsilon} \varepsilon, \quad (9)$$

where κ_{ε} is the strain coefficient of the FBG when combined with the taper, which is given by

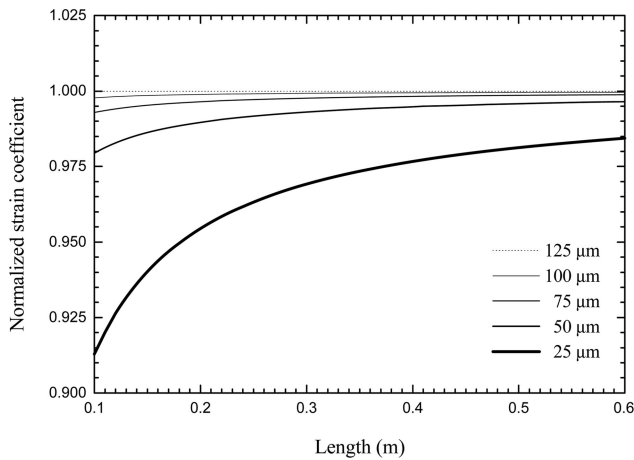


Fig. 2. Relationship between the normalized strain coefficient (relative to the case of the nontapered fiber section) with the total length of the sensing head.

$$\kappa_{\varepsilon} = \kappa_{\varepsilon(\text{FBG})} \frac{L_{\text{FBG}} + L_{\text{taper}} + L_{\text{fiber}}}{L_{\text{FBG}} + L_{\text{taper}} \left(\frac{d_{\text{FBG}}}{d_{\text{taper}}} \right)^2 + L_{\text{fiber}}} \quad (10)$$

Figure 2 shows the dependence of the FBG strain coefficient on the total length of the sensing head for different diameters of the fused taper. The presented results are normalized to the simple FBG strain coefficient, $\kappa_{\varepsilon(\text{FBG})}$. It can be seen that a large reduction of the fused taper diameter results in a significant decrease in the strain sensitivity of the FBG sensor, which is even more dramatic for smaller lengths of the sensing head.

3. Experimental Results

To perform this experiment, three sensing head structures similar to the one shown in Fig. 1 were implemented. They consist of a single FBG structure with a length of 10 mm in series with a fused taper. The spacing between these elements is approximately 50 mm. The FBGs were written in single-mode fiber (SMF28) by UV exposure through a phase

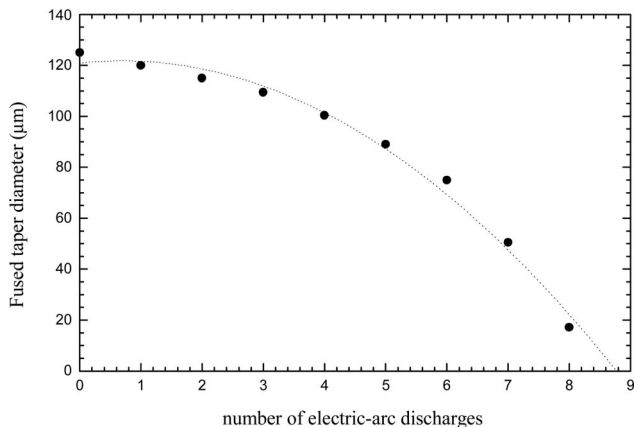


Fig. 3. Fused taper diameter versus number of electric discharges.

mask using an excimer laser operating at 248 nm ($\lambda_B \approx 1550$ nm). The three sensing heads were fabricated with different taper diameters. The fused tapers were fabricated by elongating the fiber during an electric-arc discharge, which was provided by a splicing machine. The electric arc is characterized by an electric current of 9 mA and arc duration of 1 s.

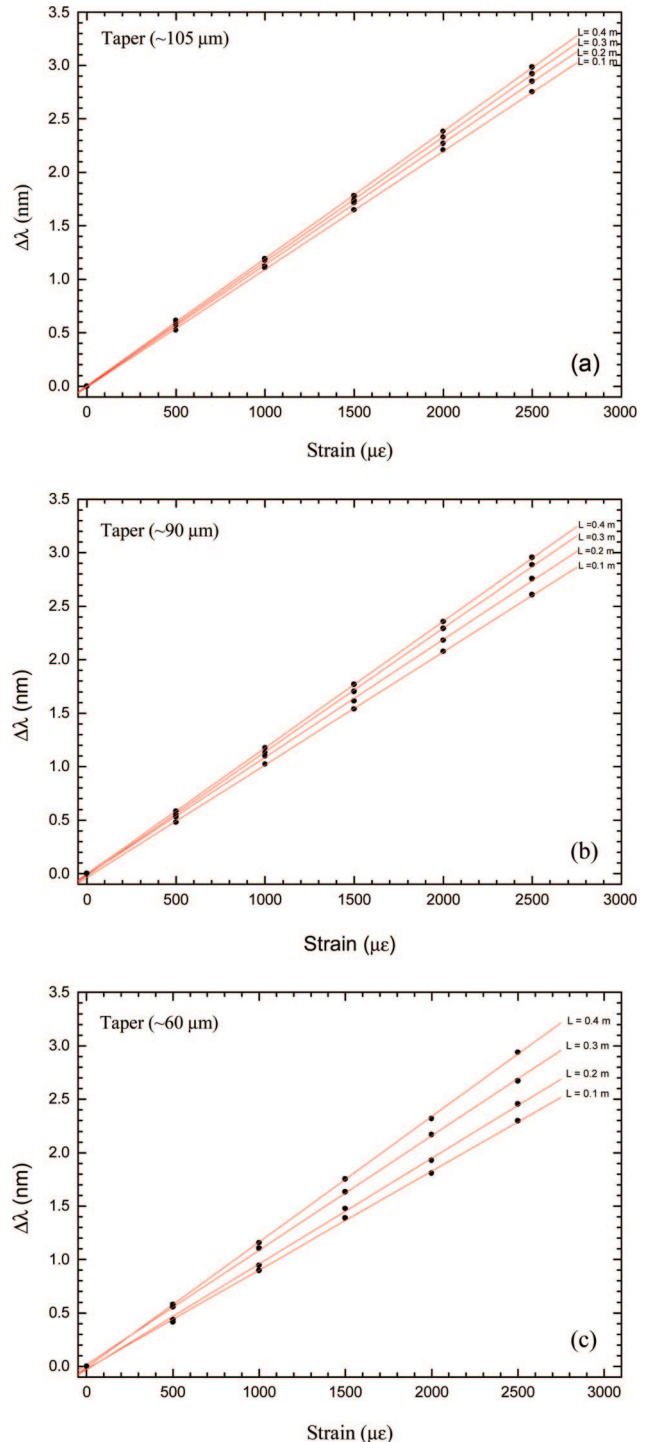


Fig. 4. (Color online) Strain response of the FBG in a sensing head with different gauge lengths and in series with a fiber fused taper with diameters of (a) 105, (b) 90, and (c) 60 μm .

The fabrication parameters of the tapers were adjusted to decrease the fiber diameter from 125 to 105, 90, and 60 μm in the three taper waists. The resulting taper structures have a total average length of $\sim 500 \mu\text{m}$ and an average insertion loss of $\sim 0.1 \text{ dB}$ for all tapers used in this experiment. The fused taper diameter depends on the number of electric-arc discharges. Figure 3 shows the relationship between the number of electric-arc discharges and the taper diameter. The nonlinear response depends on the elongation per electric-arc discharge increasing due to the subsequent decrease of the taper waist.

The sensing head was interrogated using a conventional setup consisting of a broadband source, an optical circulator, and an optical spectrum analyzer. The optical source is an erbium-doped broadband source with a spectral bandwidth of 100 nm and a central wavelength of 1550 nm. The optical spectrum analyzer has a resolution of 0.05 nm.

Figure 4 presents the strain responses for the three sensing heads based on a single FBG combined with fused tapers with different diameters: (a) 105, (b) 90, and (c) 60 μm . The three graphics also show the strain sensitivity dependence on the strain gauge length ($L = 0.1, 0.2, 0.3,$ and 0.4 m). The results demonstrate that the dependence of the strain sensitivity on the gauge length is higher for the 60 μm taper, i.e., the grating sensitivity to applied strain decreases with the reduction of the taper diameter. This result is due to the fact that the stress is higher in the fused taper region than in the FBG region. If the sensing head is longer than 0.5 m, the effect of the fused taper region becomes negligible and the strain sensitivity is the same as for the FBG without the fused taper.

All these results are aggregated in Fig. 5, which shows the dependence of the measured FBG strain sensitivity, κ_s , on the total length of the sensing head, for three different fused taper diameters. For each case, the theoretical curve derived from Eq. (10) is also presented. Within the 3% error bar indicated, there is agreement between the experimental and the

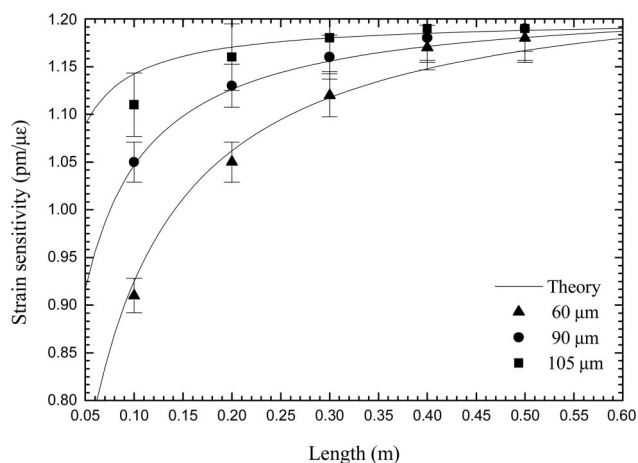


Fig. 5. Experimental and theoretical FBG strain sensitivity versus total length of the sensing head for different taper diameters.



Fig. 6. Geometry of the interferometric structure based on the fabrication of a fused taper at the middle of a FBG.

theoretical results. The error is essentially due to modification of the material properties on the fused taper region originated by the electric-arc discharge.

The strain sensitivity of the interferometric structure formed by a fused taper between two FBG-based mirrors was also investigated. For this a 10 mm length grating was written in SMF28 using an excimer laser. After the inscription, the middle of the grating was positioned in the splice machine and three discharges were made. In this way, the refractive index modulation was erased in that region and a FBG-based Fabry–Pérot structure was formed with a taper region in between (Fig. 6). Figure 7 shows the spectral response of the Bragg grating and of the interferometric structure after fabrication of the fused taper. As expected, the spectral response of the device is the convolution of the spectral response of the uniform Bragg grating with the fringe pattern of the interferometer. Also, it is observed that the width of such a spectral response is larger than that of the original grating. This is a consequence of the shorter length of the two FBG-based device mirrors.

Two main fringes are visible within the FBG envelope, with a spectral separation indicating a cavity length of $\sim 6.8 \text{ mm}$. The peak wavelengths of these fringes change with applied strain, as a consequence of the induced phase variation of the interferometric structure. Due to the presence of the taper, the slope of this variation is larger than that of the spectral envelope, which changes because the FBG mirrors also experience strain. As a result, the relative optical power of these two peaks should vary with strain. To check this, a visibility-type parameter is defined as $(R_1 - R_2)/(R_1 + R_2)$, where R_1 and R_2 are the reflectivities of the peaks indicated in Fig. 7. By the argument described previously, this change should also

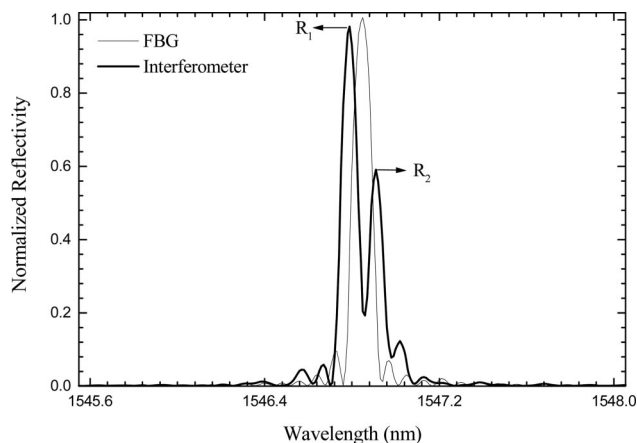


Fig. 7. Spectral response of the Bragg grating and of the structure formed after fabrication of the fused taper at the middle of the grating.

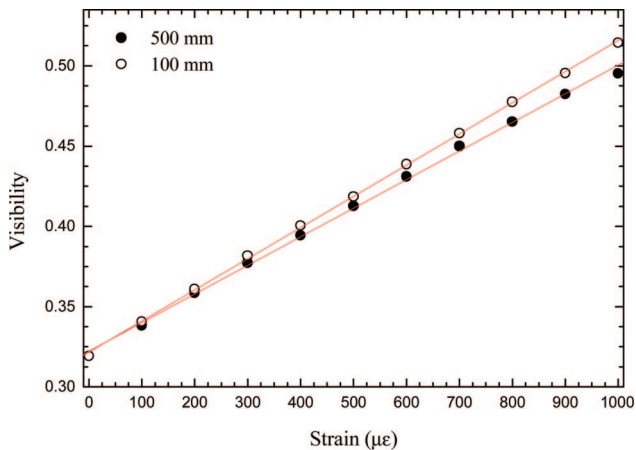


Fig. 8. (Color online) Relationship between the visibility type parameter $(R_1 - R_2)/(R_1 + R_2)$ and the strain for two gauge lengths (100 and 500 mm).

be dependent on the gauge length. This was confirmed experimentally, as shown in Fig. 8. Two gauge lengths were considered, and in both cases a linear variation with applied strain was observed in the addressed range ($1000 \mu\epsilon$), with slopes of $1.94 \times 10^{-4} \mu\epsilon^{-1}$ (100 mm) and $1.78 \times 10^{-4} \mu\epsilon^{-1}$ (500 mm). Globally, these results indicate that it is feasible to measure strain applied to the interferometric structure using the defined visibility-type parameter, with a readout sensitivity that can be tuned to a certain extent by adjusting the gauge length.

4. Conclusions

We have reported the principle, the analysis, and the experimental results of a sensing head formed by a single fiber Bragg grating in series with a fused taper. The FBG sensitivity to strain was determined by the physical dimensions of the sensor system, namely, the ratio between the radius of fiber and the fused taper, as well as the ratio between the length of the fiber and the taper. These ratios determine how the strain is distributed along the different sections of the sensor system. In particular, if the section of the fused taper is much smaller than the section with the FBG then the strain will be lower in the latter, leading to smaller deformation and, consequently, reduced sensitivity. Hence, we can customize the sensor sensitivity by carefully designing these geometric dimensions. For a taper diameter of $60 \mu\text{m}$, the strain sensitivity reduction achieved when the gauge length changes in the range of 10–50 cm reaches $\sim 23\%$ relative to the standard value obtained with a simple FBG. It should be noted that it is also feasible to increase sensitivity if, instead of including fused tapers, fiber structures with a larger diameter than the FBG are placed in series. This flexibility opens several possibilities in the conception of fiber optic sensing heads with specific characteristics as, for example, for simultaneous multiparameter measurement. The controlled reduction

of sensitivity of the sensor can be used as a possible solution when there is a large number of FBGs all positioned along a single optical fiber and we want to reduce the cross talk between them by controlling the measurement range of each FBG.

We also described the investigation performed on strain measurements using a fiber interferometer fabricated by inducing an electric-arc fused taper at the middle of a FBG. The achieved Fabry–Pérot configuration has a strain sensitivity that is also a function of the taper diameter and gauge length. A visibility-type parameter was defined, which permitted the interrogation of the sensing head and study of its strain measurement characteristics without the need of interferometric phase reading.

Another important result that we established demonstrates how we can use geometric dimensions of the sensor to customize and control its sensitivity. Though we focused on situations where the sensitivity is reduced, this approach can be used to meet other design specifications, opening the possibility for newer applications and concept designs.

References

1. Y.-L. Rao, "In-fibre Bragg grating sensors," *Meas. Sci. Technol.* **8**, 355–375 (1997).
2. B. Lee, "Review of the present status of optical fiber sensors," *Opt. Fiber Technol.* **9**, 57–79 (2003).
3. O. Frazão, L. A. Ferreira, F. M. Araújo, and J. L. Santos, "Applications of fiber optic grating technology to multi-parameter measurement," *Fiber Integ. Opt.* **24**, 227–244 (2005).
4. S. W. James, M. L. Dockney, and F. P. Tatam, "Simultaneous independent temperature and strain measurement using in-fibre Bragg grating sensors," *Electron. Lett.* **32**, 1133–1134 (1996).
5. O. Frazão, L. A. Ferreira, F. M. Araújo, and J. L. Santos, "Simultaneous measurement of strain and temperature using Bragg gratings in a twisted configuration," *J. Opt. A* **7**, 427–430 (2005).
6. O. Frazão, M. Melo, P. V. S. Marques, and J. L. Santos, "Chirped Bragg grating fabricated in fused fibre taper for strain-temperature discrimination," *Meas. Sci. Technol.* **16**, 984–988 (2005).
7. M. G. Xu, L. Dong, L. Reekie, J. A. Tucknott, and J. L. Cruz, "Temperature-independent strain sensor using a chirped Bragg grating in a tapered optical fibre," *Electron. Lett.* **31**, 823–825 (1995).
8. D. Weichong, T. Xiaoming, and T. Hwa-yaw, "Fibre Bragg grating cavity sensors for simultaneous measurement of strain and temperature," *IEEE Photon. Technol. Lett.* **11**, 105–107 (1999).
9. J. F. Ding, A. P. Zhang, L. Y. Shao, J. H. Yan, and S. He, "Fiber-taper seeded long-period grating pair as a highly sensitive refractive-index sensor," *IEEE Photon. Technol. Lett.* **17**, 1247–1249 (2005).
10. M. Song, S. B. Lee, S. S. Choi, and B. Lee, "Simultaneous measurement of temperature and strain using two fiber Bragg gratings embedded in a glass tube," *Opt. Fiber Technol.* **3**, 194–196 (1997).
11. V. V. Spirin, M. G. Shlyagin, S. V. Miridonov, and J. Marquez, "Temperature-insensitive strain measurement using differential double Bragg grating technique," *Opt. Laser Technol.* **33**, 43–46 (2001).